

# Pd- and Ru-Catalyzed Intramolecular Carbene C<sub>Ar</sub>-H Functionalization of $\gamma$ -Amino- $\alpha$ -diazoesters for the Synthesis of Tetrahydroquinolines

Daniel Solé,<sup>\*[a]</sup> Arianna Amenta,<sup>[a]</sup> M.-Lluïsa Bennasar<sup>[a]</sup> and Israel Fernández<sup>\*[b]</sup>

**Abstract:** A synthesis of tetrahydroquinoline-4-carboxylic acid esters has been developed via the transition metal-catalyzed intramolecular aromatic C–H functionalization of  $\alpha$ -diazoesters. Both [(IMes)Pd(NQ)]<sub>2</sub> and the first generation Grubbs catalyst proved effective for this purpose. The ruthenium catalyst was found to be the most versatile, although in a few cases the palladium complex afforded better yields or selectivities. According to DFT calculations, the Pd(0)- and Ru(II)-catalyzed C<sub>Ar</sub>sp<sup>2</sup>-H functionalization proceed through rather different reaction mechanisms. Thus, the Pd(0)-catalyzed reaction involves a Pd-mediated 1,6-H migration from the C<sub>Ar</sub>sp<sup>2</sup>-H bond to the carbene carbon atom, followed by a reductive elimination process. In contrast, an electrophilic addition of the ruthena-carbene intermediate to the aromatic ring and subsequent 1,2-proton migration are operative in the Grubbs catalyst-promoted reaction.

## Introduction

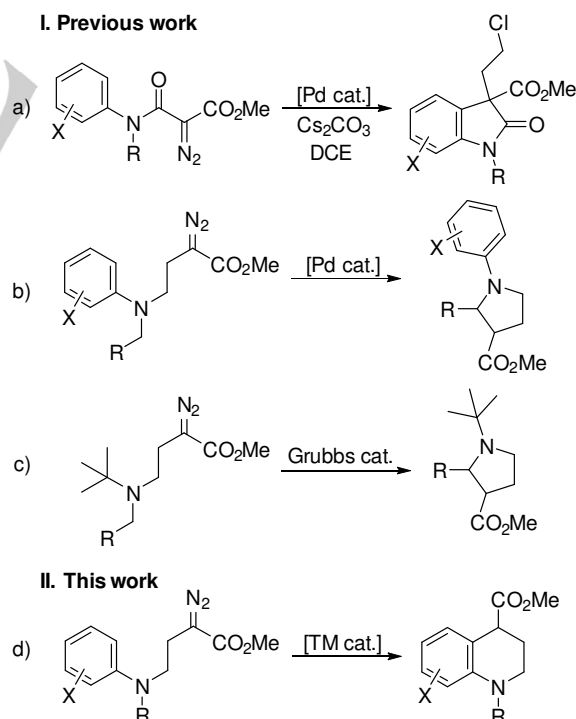
The transition metal-catalyzed intramolecular aromatic C–H functionalization of  $\alpha$ -diazocarbonyl compounds<sup>[1]</sup> constitutes a powerful method of annulation of the benzene nucleus, with considerable appeal in medicinal heterocyclic chemistry. A number of successful reactions involving the formation of [6,5]-bicycles have been reported, allowing the elaboration of both carbocyclic and heterocyclic backbones, including the oxindole,<sup>[2-5]</sup> indanone<sup>[6]</sup> and benzo- $\gamma$ -sultam systems.<sup>[7]</sup> Traditionally, these intramolecular aromatic substitution reactions from  $\alpha$ -diazocarbonyl compounds have been carried out in the presence of rhodium(II) catalysts,<sup>[2,6,7]</sup> although in recent times other transition metals, especially ruthenium,<sup>[3]</sup> have proved useful.

In contrast, the use of the intramolecular aromatic C–H functionalization of  $\alpha$ -diazocarbonyl compounds for the construction of [6,6]-bicycles has been less successful, probably because of the competition from the so-called Buchner

reaction.<sup>[8]</sup> Nevertheless, rhodium-based catalysts have been effectively applied to selectively promote intramolecular aromatic C–H functionalization of  $\alpha$ -diazo- $\beta$ -dicarbonyl compounds to construct isoquinolinones,<sup>[9]</sup> dihydroquinolinones<sup>[10]</sup> and chromanones.<sup>[11]</sup>

All the above processes, often inaccurately referred to as aromatic C–H insertions,<sup>[12]</sup> differ mechanistically from the aliphatic version in that they generally involve the electrophilic addition of the corresponding metal carbene intermediate to the aromatic ring, followed by a 1,2-proton migration.<sup>[13]</sup>

In the last years, we have been exploring the use of different transition metal catalysts as alternatives to the widely used Rh(II)-complexes<sup>[14]</sup> for carbene C–H insertion of  $\alpha$ -diazocarbonyl compounds.<sup>[15]</sup> In this context, we have reported that palladium catalysts efficiently promote carbene C<sub>Ar</sub>sp<sup>2</sup>-H functionalization of  $\alpha$ -diazo- $\beta$ -(methoxycarbonyl)acetanilides to form oxindoles through a sequential insertion/alkylation process (Scheme 1a).<sup>[16]</sup>



**Scheme 1.** Pd and Grubbs catalysts in intramolecular C–H functionalization of  $\alpha$ -diazocarbonyl compounds for heterocyclic synthesis.

Mechanistically, this palladium-catalyzed insertion is clearly different from C<sub>Ar</sub>sp<sup>2</sup>-H functionalization based on other

[a] Prof. Dr. D. Solé, A. Amenta, Prof. Dr. M.-L. Bennasar  
Laboratori de Química Orgànica, Facultat de Farmàcia i Ciències de l'Alimentació  
Universitat de Barcelona  
Av. Joan XXIII 27-31, 08028 Barcelona (Spain)  
E-mail: [dsole@ub.edu](mailto:dsole@ub.edu)

[b] Prof. Dr. I. Fernández  
Departamento de Química Orgànica I and Centro de Innovación en Química Avanzada (ORFEO-CINQA), Facultat de Ciències Químicas  
Universidad Complutense de Madrid  
28040 Madrid (Spain)  
E-mail: [israel@quim.ucm.es](mailto:israel@quim.ucm.es)  
Supporting information for this article is given via a link at the end of the document.

transition metals and involves a palladium-mediated 1,5-H migration followed by reductive elimination.

We have also studied the transition metal-catalyzed decomposition of  $\alpha$ -diaoesters.<sup>[17]</sup> Thus, we have shown that palladium catalysts are also able to promote intramolecular carbene  $Csp^3$ -H insertion of  $\gamma$ -anilino- $\alpha$ -diaoesters to produce pyrrolidines through  $Csp^3$ - $Csp^3$  bond formation (Scheme 1b). It should be noted that although the effectiveness of palladium complexes in catalyzing carbene C-H insertion reactions from  $\alpha$ -diazo carbonyl compounds was first demonstrated some time ago, there are few reports on the use of palladium catalysts in this particular kind of chemistry.<sup>[18]</sup>

More recently, we have reported the first example of an unprecedented nonmetathetic chemistry of Grubbs complexes,<sup>[19]</sup> which were applied to promote the carbene  $Csp^3$ -H insertion of  $\gamma$ -dialkylamino- $\alpha$ -diaoesters to form pyrrolidines (Scheme 1c).<sup>[20]</sup>

Continuing our program of developing efficient methodologies for the synthesis of nitrogen heterocycles,<sup>[21]</sup> we sought to explore the construction of tetrahydroquinolines by transition metal-catalyzed decomposition of  $\gamma$ -anilino- $\alpha$ -diaoesters (Scheme 1d). The extensive bioactivity of tetrahydroquinolines, including antitumor, antiviral, antibacterial, antimalarial and antifungal activity, is well documented, and the development of efficient procedures for their preparation is therefore of considerable interest.<sup>[22-23]</sup> The aim of the current work was to investigate the feasibility of using both palladium(0) and Grubbs catalysts to promote the intramolecular carbene  $C_{Ar}sp^2$ -H functionalization and to identify differences in the reactivities and selectivities between the two transition metals. Thus, herein we report a full account of our experimental and computational studies on the transition metal-catalyzed  $C_{Ar}sp^2$ -H functionalization in the search for a suitable methodology for the synthesis of tetrahydroquinolines.

## Results and Discussion

In our studies on the transition metal-catalyzed reactions of  $\gamma$ -amino- $\alpha$ -diaoesters,<sup>[17b]</sup> we found that the use of either  $Pd_2(dba)_3$  or  $[(IMes)Pd(NQ)]_2$  as catalysts to promote the decomposition of *N*-isopropyl  $\alpha$ -diaoester **1a** resulted in the chemoselective functionalization at the aryl  $Csp^2$ -H bond to give tetrahydroquinoline **2a** (Table 1, entries 1-2). With these data in hand, we began by testing the use of Grubbs catalysts **Ru-1**, **Ru-2** and **Ru-3** (Figure 1) to promote the annulation reaction from **1a**. Gratifyingly, treatment of **1a** with first generation Grubbs catalyst **Ru-1** resulted in the chemoselective formation of **2a** in good yield (entry 3). Similar chemoselectivity and a slightly lower yield were observed with second generation Grubbs catalyst **Ru-2** (entry 4), but when Hoveyda-Grubbs catalyst **Ru-3** was used, competition from the  $Csp^3$ -H insertion led to the formation of significant amounts of pyrrolidine **3a** (entry 5).

In order to investigate the scope of the  $C_{Ar}sp^2$ -H functionalization reaction for the preparation of tetrahydroquinoline-4-carboxylic acid esters,  $Pd_2(dba)_3$ ,  $[(IMes)Pd(NQ)]_2$  and **Ru-1** were tested as catalysts with a variety

of substituted  $\gamma$ -anilino- $\alpha$ -diaoesters bearing different substituents at the aromatic ring as well as at the nitrogen atom.

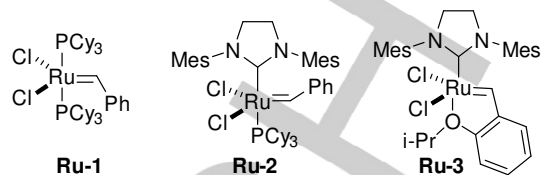
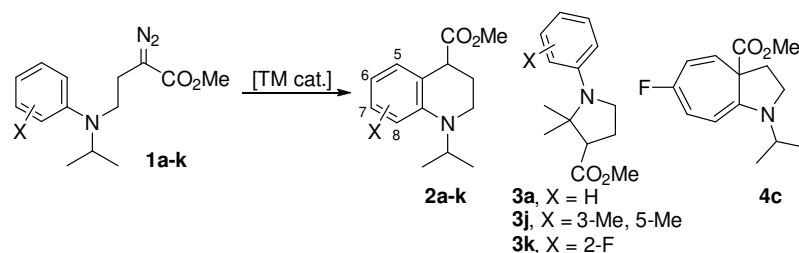


Figure 1. Commonly used Grubbs catalysts.

The examples in Tables 1 and 2 confirm the generality and functional group tolerance of these reactions. As can be seen in Table 1, no competition from the  $Csp^3$ -H insertion was observed when starting from *para*- and *meta*-substituted *N*-isopropylanilines (entries 6-25). Thus, when using either  $[(IMes)Pd(NQ)]_2$  or **Ru-1** as catalysts, the *para*-substituted anilines **1b-d** (entries 6-14) chemoselectively underwent  $C_{Ar}sp^2$ -H functionalization to give the corresponding tetrahydroquinolines regardless of the nature of the substituent. In contrast, whereas the use of  $Pd_2(dba)_3$  selectively led to tetrahydroquinolines **2b** and **2d** (entries 6 and 12), when starting from the *para*-fluoro aniline **1c**, a mixture of tetrahydroquinoline **2c** and the Buchner product **4c** was observed (entry 9). For *para*-substituted anilines, **Ru-1** invariably afforded the best results whereas the least efficient catalyst was  $Pd_2(dba)_3$ .

*meta*-Substituted anilines **1e-i** also underwent chemoselective  $C_{Ar}sp^2$ -H functionalization to give the corresponding tetrahydroquinolines with either the  $Pd(0)$ - or **Ru-1** catalysts, the latter once again affording the highest reaction yields (entries 15-25). With these substrates, the regioselectivity of the insertion (5-X/7-X ratio) seems to be controlled by a combination of steric and electronic effects. Thus, similar moderate regioselectivities were obtained in the reactions of anilines **1e** and **1f**, which bear a *m*-methoxy and *m*-chloro substituent, respectively, using either  $[(IMes)Pd(NQ)]_2$  or **Ru-1** (entries 15-19). However, with the *m*-iodo substituted aniline **1g**, the  $Pd(0)$ -catalyst afforded better regioselectivity than **Ru-1** (entries 20-21). On the other hand, in the reactions of anilines **1h** and **1i**, which bear the highly electron-withdrawing groups *m*- $CO_2Me$  and *m*- $NO_2$ , respectively, almost complete regioselectivity was observed with both  $[(IMes)Pd(NQ)]_2$  and **Ru-1** (entries 22-25).

The  $C_{Ar}sp^2$ -H functionalization from dimethylaniline **1j** was also selectively promoted by  $[(IMes)Pd(NQ)]_2$ , while the use of **Ru-1** led to the formation of significant amounts of pyrrolidine **3j**, resulting from the  $Csp^3$ -H insertion (entries 26-27). In contrast, competition between  $C_{Ar}sp^2$ -H and  $Csp^3$ -H insertion was observed in the reactions of *ortho*-fluoroaniline **1k** in the presence of  $[(IMes)Pd(NQ)]_2$  or **Ru-1** catalysts (entries 28-29). Interestingly, as in the reaction of **1j**, tetrahydroquinoline formation was enhanced by the use of the  $Pd(0)$ -catalyst, which afforded a 1:1 mixture of **2k** and **3k**. The high tendency of *ortho*-substituted aniline **1k** to undergo  $Csp^3$ -H functionalization, which is in line with our previously reported results,<sup>[17a-b]</sup> can be mainly ascribed to steric factors.

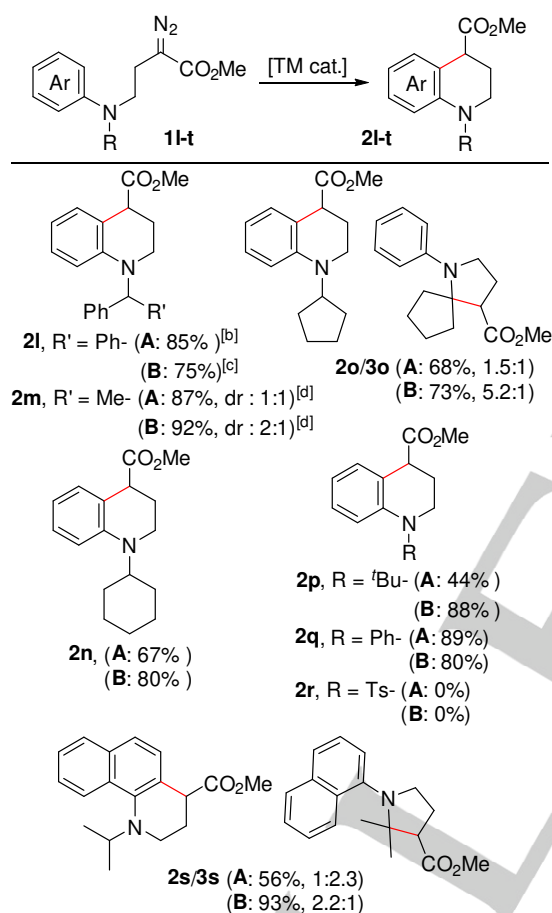
**Table 1.** Transition metal-catalyzed  $C_{Ar}sp^2$ -H functionalization of  $\alpha$ -diazooesters **1a-k**.

Entry	<b>1</b> (X)	[TM cat.]	Products (yield) <sup>[a]</sup>
1	<b>1a</b> (H)	$Pd_2(dba)_3$ <sup>[b]</sup>	<b>2a</b> , X = H (80%) <sup>[e]</sup>
2	<b>1a</b> (H)	$[(IMes)Pd(NQ)]_2$ <sup>[c]</sup>	<b>2a</b> , X = H (75%) <sup>[e]</sup>
3	<b>1a</b> (H)	<b>Ru-1</b> <sup>[d]</sup>	<b>2a</b> , X = H (82%)
4	<b>1a</b> (H)	<b>Ru-2</b> <sup>[d]</sup>	<b>2a</b> , X = H (68%)
5	<b>1a</b> (H)	<b>Ru-3</b> <sup>[d]</sup>	<b>2a</b> , X = H/ <b>3a</b> (3:1, 53%)
6	<b>1b</b> (4-Me)	$Pd_2(dba)_3$ <sup>[b]</sup>	<b>2b</b> , X = 6-Me (64%)
7	<b>1b</b> (4-Me)	$[(IMes)Pd(NQ)]_2$ <sup>[c]</sup>	<b>2b</b> , X = 6-Me (70%)
8	<b>1b</b> (4-Me)	<b>Ru-1</b> <sup>[d]</sup>	<b>2b</b> , X = 6-Me (87%)
9	<b>1c</b> (4-F)	$Pd_2(dba)_3$ <sup>[b]</sup>	<b>2c</b> , X = 6-F (38%)/ <b>4c</b> (15%)
10	<b>1c</b> (4-F)	$[(IMes)Pd(NQ)]_2$ <sup>[c]</sup>	<b>2c</b> , X = 6-F (68%)
11	<b>1c</b> (4-F)	<b>Ru-1</b> <sup>[d]</sup>	<b>2c</b> , X = 6-F (97%)
12	<b>1d</b> (4-OMe)	$Pd_2(dba)_3$ <sup>[b]</sup>	<b>2d</b> , X = 6-OMe (55%)
13	<b>1d</b> (4-OMe)	$[(IMes)Pd(NQ)]_2$ <sup>[c]</sup>	<b>2d</b> , X = 6-OMe (69%)
14	<b>1d</b> (4-OMe)	<b>Ru-1</b> <sup>[d]</sup>	<b>2d</b> , X = 6-OMe (88%)
15	<b>1e</b> (3-OMe)	$Pd_2(dba)_3$ <sup>[b]</sup>	<b>2e</b> , X = 7-OMe/X = 5-OMe (40%, 3.7:1)
16	<b>1e</b> (3-OMe)	$[(IMes)Pd(NQ)]_2$ <sup>[c]</sup>	<b>2e</b> , X = 7-OMe/X = 5-OMe (70%, 3.7:1)
17	<b>1e</b> (3-OMe)	<b>Ru-1</b> <sup>[d]</sup>	<b>2e</b> , X = 7-OMe/X = 5-OMe (86%, 3.7:1)
18	<b>1f</b> (3-Cl)	$[(IMes)Pd(NQ)]_2$ <sup>[c]</sup>	<b>2f</b> , X = 7-Cl/X = 5-Cl (68%, 3:1)
19	<b>1f</b> (3-Cl)	<b>Ru-1</b> <sup>[d]</sup>	<b>2f</b> , X = 7-Cl/X = 5-Cl (82%, 3:1)
20	<b>1g</b> (3-I)	$[(IMes)Pd(NQ)]_2$ <sup>[c]</sup>	<b>2g</b> , X = 7-I/X = 5-I (70%, 8.5:1)
21	<b>1g</b> (3-I)	<b>Ru-1</b> <sup>[d]</sup>	<b>2g</b> , X = 7-I/X = 5-I (81%, 3.5:1)
22	<b>1h</b> (3-CO <sub>2</sub> Me)	$[(IMes)Pd(NQ)]_2$ <sup>[c]</sup>	<b>2h</b> , X = 7-CO <sub>2</sub> Me/X = 5-CO <sub>2</sub> Me (75%, >19:1)
23	<b>1h</b> (3-CO <sub>2</sub> Me)	<b>Ru-1</b> <sup>[d]</sup>	<b>2h</b> , X = 7-CO <sub>2</sub> Me/X = 5-CO <sub>2</sub> Me (90%, >19:1)
24	<b>1i</b> (3-NO <sub>2</sub> )	$[(IMes)Pd(NQ)]_2$ <sup>[c]</sup>	<b>2i</b> , X = 7-NO <sub>2</sub> /X = 5-NO <sub>2</sub> (48%, >19:1)
25	<b>1i</b> (3-NO <sub>2</sub> )	<b>Ru-1</b> <sup>[d]</sup>	<b>2i</b> , X = 7-NO <sub>2</sub> /X = 5-NO <sub>2</sub> (94%, >19:1)
26	<b>1j</b> (3-Me, 5-Me)	$[(IMes)Pd(NQ)]_2$ <sup>[c]</sup>	<b>2j</b> , X = 5-Me, 7-Me (82%)
27	<b>1j</b> (3-Me, 5-Me)	<b>Ru-1</b> <sup>[d]</sup>	<b>2j</b> , X = 5-Me, 7-Me/ <b>3j</b> (3:1, 88%)
28	<b>1k</b> (2-F)	$[(IMes)Pd(NQ)]_2$ <sup>[c]</sup>	<b>2k</b> , X = 8-F/ <b>3k</b> (1:1, 64%)
29	<b>1k</b> (2-F)	<b>Ru-1</b> <sup>[d]</sup>	<b>2k</b> , X = 8-F/ <b>3k</b> (1:3.5, 98%)

[a] Yields refer to products isolated by chromatography and for entries in which a product mixture was obtained, the yield refers to the combined yield. [b] Catalyst (5 mol%) in DCE at reflux for 24 h. [c] Catalyst (2.5 mol%) in CHCl<sub>3</sub> at reflux for 24 h. [d] Catalyst (3 mol%) in CH<sub>2</sub>Cl<sub>2</sub> at reflux for 24 h. [e] See ref. 17b.

The  $C_{Ar}sp^2$ -H functionalization was not limited to *N*-isopropylanilines but also proved suitable for anilines bearing other substituents at the nitrogen atom (Table 2). Thus, *N*-benzhydrylaniline **1l** chemoselectively afforded tetrahydroquinoline **2l** in 85% and 75% reaction yield in the presence of  $[(IMes)Pd(NQ)]_2$  or **Ru-1**, respectively. Similarly, the reaction of *N*-(1-phenylethyl)aniline **1m** in the presence of either  $[(IMes)Pd(NQ)]_2$  or **Ru-1** chemoselectively afforded tetrahydroquinoline **2m** (mixture of stereoisomers) in good yields.

**Table 2.** Transition metal-catalyzed  $C_{Ar}sp^2$ -H functionalization of  $\alpha$ -diazooesters **1l-1t**.<sup>[a]</sup>



[a] Yields refer to products isolated by chromatography and for entries in which a product mixture was obtained, the yield refers to the combined yield. [b] A:  $[(IMes)Pd(NQ)]_2$  (2.5 mol%) in  $CHCl_3$  at reflux for 24 h. [c] B: **Ru-1** (3 mol%) in  $CH_2Cl_2$  at reflux for 24 h. [d] dr = diastereomeric ratio.

Both catalysts selectively promoted  $C_{Ar}sp^2$ -H functionalization of *N*-cyclohexylaniline **1n** to give **2n**, and although their use with *N*-cyclopentylaniline **1o** led to mixtures of tetrahydroquinoline **2o** and spirocyclic pyrrolidine **3o**, the former was obtained in an acceptable yield of 61% when using **Ru-1**. In the presence of either  $[(IMes)Pd(NQ)]_2$  or **Ru-1**, *N*-*tert*-butyl  $\alpha$ -diazooester **1p** and *N,N*-diphenyl  $\alpha$ -diazooester **1q** also underwent  $C_{Ar}sp^2$ -H functionalization to give tetrahydroquinolines **2p** and **2q**, respectively, in good yields. However, both catalysts failed to

promote the C-H functionalization reaction of *p*-toluene sulfonamide **1r**. On the other hand, in the reaction of  $\alpha$ -diazooester **1s** the use of **Ru-1** afforded tetrahydrobenzo[*h*]quinolone **2s** in 64%, whereas  $[(IMes)Pd(NQ)]_2$  reversed the regioselectivity, providing pyrrolidine **3s** as the main product together with minor amounts of **2s**.

To shed light on the reaction mechanism and selectivity of the Pd(0)- and Grubbs catalyst-promoted functionalizations described above, density functional theory (DFT) calculations were carried out.<sup>[24]</sup> To this end, we first explored the process involving **1a** which, in the presence of  $[(IMes)Pd(NQ)]_2$ , leads to the formation of tetrahydroquinoline **2a** (see entry 2, Table 1). Similar to related Pd(0)-mediated C-H insertions of  $\alpha$ -diazocarbonyl compounds,<sup>[16-17]</sup> our calculations started from the corresponding pallada(0)-carbene intermediate **INT0**, formed by the reaction of the diazo compound **1a** and a model Pd(0)-catalyst where the bulky mesyl groups in the NHC ligand were replaced by phenyl groups. This species evolves into the seven-membered palladacycle **INT1** through the transition state **TS1** in a highly exergonic transformation ( $\Delta G_R = -25.3$  kcal/mol). As shown in Figure 2, this saddle point is associated with a Pd-mediated 1,6-H migration from the phenyl group to the carbene carbon atom which results in the formal oxidation of the transition metal. Then, **INT1** is transformed into the observed tetrahydroquinoline **2a** through a reductive elimination reaction via **TS2**. This final exergonic step ( $\Delta G_R = -10.4$  kcal/mol) forms the new C-C bond and releases the active catalytic species Pd(NHC), which is then able to enter in a new catalytic cycle. We also explored the possible  $Csp^3$ -H activation from the initial pallada(0)-carbene. A similar Pd-mediated 1,5-H migration was found, leading to the corresponding six-membered palladacycle **INT1'**. However, the associated activation barrier involving **TS1'** is clearly much higher than that computed for the  $C_{Ar}sp^2$ -H activation involving **TS1** ( $\Delta\Delta G^\ddagger = 8.9$  kcal/mol), which is fully consistent with the complete selectivity observed experimentally (see Table 1).

The process affording the same tetrahydroquinoline (**2a**) from **1a** mediated by the first generation Grubbs catalyst (Table 1, entry 3) was studied next. Similar to the above Pd-mediated transformation and related  $Csp^3$ -H activations promoted by this Ru-catalyst,<sup>[20]</sup> our calculations also start from the analogous ruthenacarbene **INT0-Ru** (in which the bulky  $PCy_3$  phosphine ligand was replaced by  $PMe_3$ , see Figure 3).<sup>[25]</sup> We located a similar Ru-assisted 1,6-H migration reaction. However, the rather high barrier required to reach the corresponding transition state (**TS1''-Ru**,  $\Delta G^\ddagger = 56.4$  kcal/mol) makes this reaction unfeasible. Alternatively, we found that **INT0-Ru** can easily evolve (computed barrier of only 5.5 kcal/mol) into the bicyclic intermediate **INT1-Ru** via **TS1-Ru**. This saddle point is associated with the formation of the new C-C bond and this reaction step can therefore be viewed as an electrophilic addition of the metal carbene intermediate to the aromatic ring in a typical  $S_EAr$  reaction. Intermediate **INT1-Ru** is then transformed into the observed reaction product **2a** through a direct 1,2-proton migration via **TS2-Ru**, which releases the

active Ru-catalyst in a highly exergonic transformation ( $\Delta G_R = -41.0$  kcal/mol). Another alternative is that this 1,2-proton migration can proceed stepwise with the assistance of a chloride ligand attached to the transition metal. Thus, the proton first

migrates to the chloride ligand via **TS2'-Ru** forming **INT2-Ru**, and then moves to its final position, affording **2a** via **TS3-Ru**. Not surprisingly, our calculations indicate that the chloride-assisted proton transfer is slightly favored over the direct 1,2-migration.

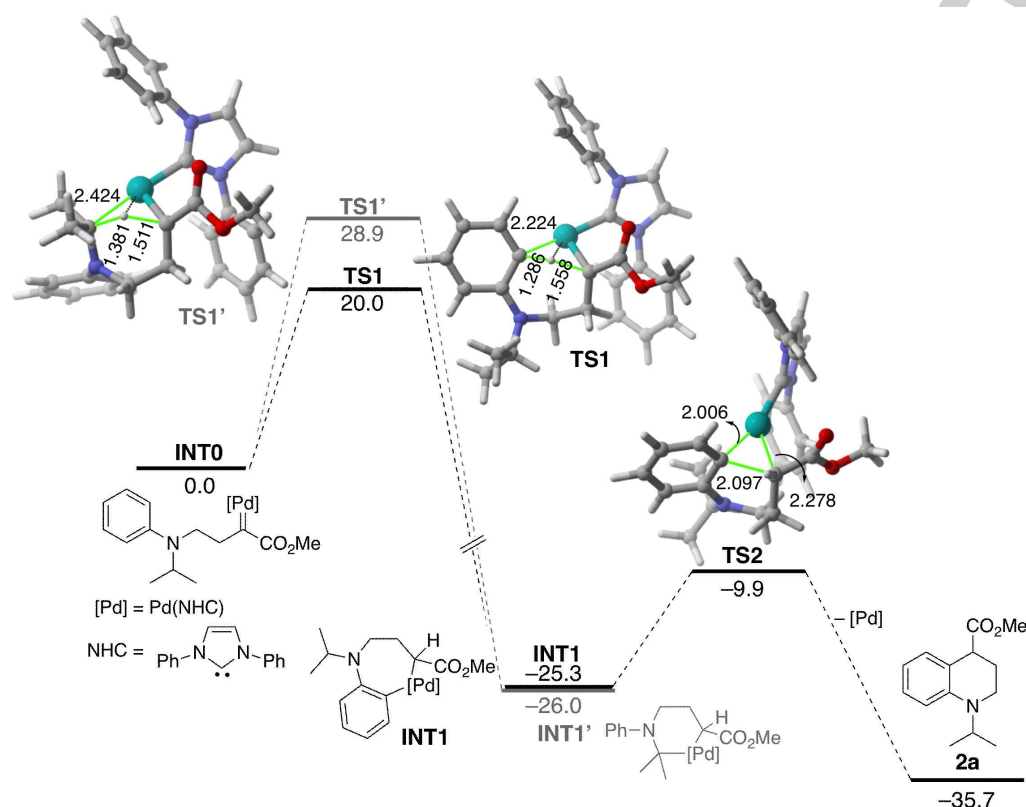


**Figure 2.** Computed reaction profile for the formation of tetrahydroquinoline **2a** mediated by the Pd(0)-catalyst. Relative free energies ( $\Delta G_{298}$ , at 298 K) and bond distances are given in kcal/mol and angstroms, respectively. All data were computed at the PCM(CHCl<sub>3</sub>)-B3LYP-D3/def2-TZVPP//PCM(CHCl<sub>3</sub>)-B3LYP-D3/def2-SVP level.

Finally, we also considered the possible  $Csp^3$ -H activation from the **INT0-Ru**, which proceeds via the expected Ru-assisted 1,5-H migration reaction. Once again, the barrier associated with reaching the corresponding saddle point **TS1'-Ru** ( $\Delta G^\ddagger = 14.4$  kcal/mol) is found to be much higher than that involving **TS1-Ru** ( $\Delta\Delta G^\ddagger = 8.9$  kcal/mol), which renders this alternative  $Csp^3$ -H activation kinetically noncompetitive, as experimentally observed.

## Conclusion

In summary, we herein report our studies on the implementation of the transition metal-catalyzed intramolecular carbene C-H functionalization of  $\alpha$ -diazoesters for the preparation of tetrahydroquinolines. Although Pd(0)- and Grubbs catalysts proved effective for this purpose, the first generation Grubbs

catalyst was more versatile, despite not always afforded the highest yields or selectivities. Starting from *N*-isopropylaniline substrates the insertion occurred selectively on the  $C_{Ar}sp^2$ -H bond to give the tetrahydroquinoline-4-carboxylic acid esters in good yields. The reaction was not limited to substrates with an *N*-isopropyl group but also proved suitable for anilines bearing other secondary alkyl groups at the nitrogen atom, as well as for the *N*-*tert*-butyl and *N*-phenyl anilines. According to DFT calculations, the mechanism involved in the  $C_{Ar}sp^2$ -H functionalization process strongly depends on the nature of the transition metal. Whereas the Pd(0)-catalyzed reaction involves a Pd-mediated 1,6-H migration from the  $C_{Ar}sp^2$ -H bond to the carbene carbon atom, followed by a reductive elimination process, in the Grubbs catalyst-promoted reaction an initial electrophilic addition of the ruthena-carbene intermediate to the aromatic ring and subsequent 1,2-proton migration are operative.

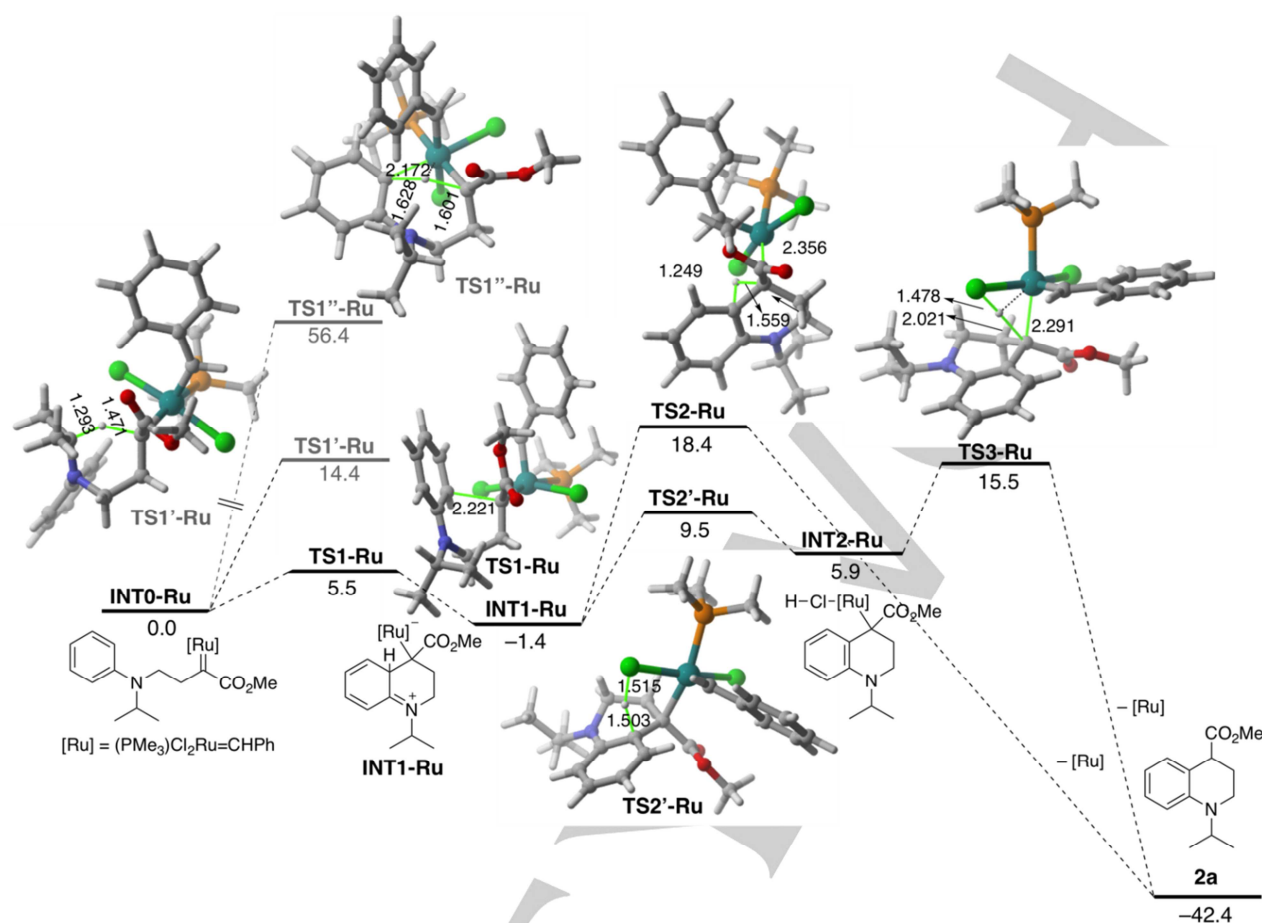


**Figure 3.** Computed reaction profile for the formation of tetrahydroquinoline **2a** mediated by the ruthenium catalyst. Relative free energies ( $\Delta G_{298}$ , at 298 K) and bond distances are given in kcal/mol and angstroms, respectively. All data were computed at the PCM( $\text{CH}_2\text{Cl}_2$ )-B3LYP-D3/def2-TZVPP//PCM( $\text{CH}_2\text{Cl}_2$ )-B3LYP-D3/def2-SVP level.

## Experimental Section

**Representative procedure for the C–H insertion reaction (Table 1, Entry 3).** A mixture of diazoester **1a** (50 mg, 0.19 mmol) and **Ru-1** (4.7 mg, 0.0057 mmol) in dichloromethane (10 mL) was stirred at reflux under an Argon atmosphere for 24 h. The solvent was removed *in vacuo*, and the residue was purified by chromatography ( $\text{SiO}_2$ , from hexanes to hexanes-EtOAc 97:3) to give **2a** (44.6 mg, 82%).

**Computational Details.** All the calculations reported in this paper were performed with the Gaussian 09 suite of programs.<sup>[26]</sup> Electron correlation was partially taken into account using the hybrid functional usually denoted as B3LYP<sup>[27]</sup> in conjunction with the D3 dispersion correction suggested by Grimme et al.<sup>[28]</sup> using the standard double- $\zeta$  quality def2-SVP<sup>[29]</sup> basis set for all atoms. The Polarizable Continuum Model (PCM)<sup>[30]</sup> was used to model the effects of the solvent. This level is denoted PCM(solvent<sub>2</sub>)-B3LYP-D3/def2-SVP. Geometries were fully optimized in solution without any geometry or symmetry constraints. Reactants, intermediates, and products were characterized by frequency calculations,<sup>[31]</sup> and have positive definite Hessian matrices. Transition structures (TS's) show only one negative eigenvalue in their diagonalized force constant matrices, and their associated eigenvectors were confirmed to correspond to the motion along the reaction coordinate

under consideration using the Intrinsic Reaction Coordinate (IRC) method.<sup>[32]</sup> Frequency calculations were also used to determine the difference between the potential ( $E$ ) and Gibbs ( $G$ ) energies,  $G - E$ , which contains the zero-point, thermal, and entropy energies. Potential energies were refined,  $E_{\text{sol}}$ , by means of single point (SP) calculations at the same level with a larger basis set, def2-TZVPP,<sup>[29]</sup> where all elements were described with a triple- $\zeta$  plus polarization quality basis set. This level is denoted PCM(solvent)-B3LYP-D3/def2-TZVPP//PCM(solvent)-B3LYP-D3/def2-SVP. The  $\Delta G$  and  $\Delta G^\ddagger$  values given in the text were obtained from the Gibbs energy in solution,  $G_{\text{sol}}$ , which was calculated by adding the thermochemistry corrections,  $G - E$ , to the refined SP energies,  $E_{\text{sol}}$ , i.e.,  $G_{\text{sol}} = E_{\text{sol}} + G - E$ .

## Acknowledgements

We gratefully acknowledge financial support for this work from MINECO-FEDER (Projects CTQ2015-64937-R, CTQ2016-78205-P, CTQ2016-81797-REDC and RTI2018-09394-B-I00).

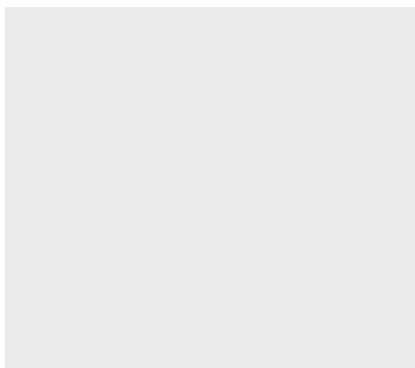
**Keywords:** diazo compounds • palladium-catalysis • ruthenium-catalysis • aromatic functionalization • density functional theory calculations

- [1] A. Ford, H. Miel, A. Ring, C. N. Slattery, A. R. Maguire, M. A. McKervey, *Chem. Rev.* **2015**, *115*, 9981-10080.
- [2] a) M. P. Doyle, M. S. Shanklin, H. Q. Pho, S. N. Mahapatro, *J. Org. Chem.* **1988**, *53*, 1017-1022; b) H. Qiu, M. Li, L.-Q. Jiang, F.-P. Lv, L. Zan, C.-W. Zhai, M. P. Doyle, W.-H. Hu, *Nat. Chem.* **2012**, *4*, 733-738; c) L.-H. Chen, Y.-T. Ma, F. Yang, X.-Y. Huang, S.-W. Chen, K. Ji, Z.-S. Chen, *Adv. Synth. Catal.* **2019**, *361*, 1307-1312.
- [3] a) W.-W. Chan, T.-L. Kwong, W.-Y. Yu, *Org. Biomol. Chem.* **2012**, *10*, 3749-3755; b) N. Liu, Q.-P. Tian, Q. Yang, S.-D. Yang, *Synlett*, **2016**, 2621-2625; c) K. Yamamoto, Z. Qureshi, J. Tsoung, G. Pisella, M. Lautens, *Org. Lett.* **2016**, *18*, 4954-4957.
- [4] H.-L. Wang, Z. Li, G.-W. Wang, S.-D. Yang, *Chem. Commun.*, **2011**, *47*, 11336-11338.
- [5] S. I. Son, W. K. Lee, J. Choi, H.-J. Ha, *Green Chem.*, **2015**, *17*, 3306-3309.
- [6] N. Watanabe, Y. Ohtake, S.-I. Hashimoto, M. Shiro, S. Ikegami, *Tetrahedron Lett.* **1995**, *36*, 1491-1494.
- [7] Z. Yang, J. Xu, *Chem. Commun.*, **2014**, *50*, 3616-1618.
- [8] See for example: K.-H. Chen, Y.-J. Chiang, J.-L. Zhu, *Org. Biomol. Chem.* **2018**, *16*, 8353-8364.
- [9] C. P. Park, A. Nagle, C. H. Yoon, C. Chen, K. W. Jung, *J. Org. Chem.* **2009**, *74*, 6231-6236.
- [10] B. Ma, F.-L. Chen, X.-Y. Xu, Y.-N. Zhang, L.-H. Hu, *Adv. Synth. Catal.* **2014**, *356*, 416-420.
- [11] X. Zhang, M. Lei, Y.-N. Zhang, L.-H. Hu, *Tetrahedron* **2014**, *70*, 3400-3406.
- [12] Y.-P. Li, Z.-Q. Li, S.-F. Zhu, *Tetrahedron Lett.* **2018**, *59*, 2307-2316.
- [13] a) S. Jia, D. Xing, D. Zhang, W. Hu, *Angew. Chem. Int. Ed.* **2014**, *53*, 13098-13101; b) C. Zheng, S.-L. You, *RSC Adv.* **2014**, *4*, 6173-6214.
- [14] a) M. P. Doyle, R. Duffy, M. Ratnikov, L. Zhou, *Chem. Rev.*, **2010**, *110*, 704-724; b) H. M. L. Davies, B. T. Parr, *Rhodium Carbenes, in Contemporary Carbene Chemistry*, R. A. Moss, M. P. Doyle, Eds., John Wiley & Sons: Hoboken, NJ, 2014, pp 363-403.
- [15] D. Solé, F. Pérez-Janer, M.-L. Bannasar, I. Fernández, *Eur. J. Org. Chem.* **2018**, 4446-4455.
- [16] D. Solé, F. Pérez-Janer, I. Fernández, *Chem. Commun.*, **2017**, *53*, 3110-3113.
- [17] a) D. Solé, F. Mariani, M.-L. Bannasar, I. Fernández, *Angew. Chem. Int. Ed.* **2016**, *55*, 6467-6470; b) D. Solé, A. Amenta, F. Mariani, M.-L. Bannasar, I. Fernández, *Adv. Synth. Catal.* **2017**, *359*, 3654-3664.
- [18] a) D. F. Taber, J. C. Amedio Jr., R. G. Sherill, *J. Org. Chem.* **1986**, *51*, 3382-3384; b) M. Matsumoto, N. Watanabe, H. Kobayashi, *Heterocycles* **1987**, *26*, 1479-1482; c) M. L. Rosenberg, J. H. F. Aasheim, M. Trebbin, E. Uggerud, T. Hansen, *Tetrahedron Lett.* **2009**, *50*, 6506-6509.
- [19] a) B. Alcaide, P. Almendros, A. Luna, *Chem. Rev.*, **2009**, *109*, 3817-3858; b) S. Kotha, S. Misra, G.; Sreevani, B. V. Babu, *Curr. Org. Chem.*, **2013**, *17*, 2776-2795.
- [20] D. Solé, A. Amenta, M.-L. Bannasar, I. Fernández, *Chem. Commun.*, **2019**, *55*, 1160-1163.
- [21] a) D. Solé, I. Fernández, *Acc. Chem. Res.* **2014**, *47*, 168-179; b) D. Solé, F. Pérez-Janer, R. Mancuso, *Chem. Eur. J.* **2015**, *21*, 4580-4584; c) D. Solé, F. Pérez-Janer, E. Zulaica, J. F. Guastavino, I. Fernández, *ACS Catal.* **2016**, *6*, 1691-1700.
- [22] a) V. Sridharan, P. A. Suryavanshi, J. C. Menéndez, *Chem. Rev.* **2011**, *111*, 7157-7259; b) I. Muthukrishnan, V. Sridharan, J. C. Menéndez, *Chem. Rev.* **2019**, *119*, 5057-5191.
- [23] Tetrahydroquinoline-4-carboxylic acid esters have shown activity as neurotropic agents<sup>[23a]</sup> and have potential therapeutic uses for some metabolic disorders.<sup>[23b-c]</sup> See, for example: a) N. Goli, P. S. Mainkar, S. S. Kotapalli, K. Tejaswini, R. Ummanni, S. Chandrasekhar, *Bioorg. Med. Chem. Lett.* **2017**, *27*, 1714-1720; b) C. Bissantz, H. Dehmlow, R. E. Martin, U. Obst Sander, H. Richter, C. Ullmer, U.S. Pat. Appl. Publ. US 20100105906 A1 20100429; c) R. Milanova, U.S. Pat. Appl. Publ. US 20060020135 A1 20060126.
- [24] All the calculations described in this work were carried out at the PCM(solvent)-B3LYP-D3/def2-TZVPP//PCM(solvent)-B3LYP-D3/def2-SVP level. See computational details.
- [25] The replacement of the PCy<sub>3</sub> ligand by PMe<sub>3</sub> has been proven to have an almost negligible influence on the computed relative free energies in a similar transformation. See reference [20].
- [26] Gaussian 09, Revision D.01, M. J. Frisch, G. W. Trucks, H. B. Schlegel, G. E. Scuseria, M. A. Robb, J. R. Cheeseman, G. Scalmani, V. Barone, B. Mennucci, G. A. Petersson, H. Nakatsuji, M. Caricato, X. Li, H. P. Hratchian, A. F. Izmaylov, J. Bloino, G. Zheng, J. L. Sonnenberg, M. Hada, M. Ehara, K. Toyota, R. Fukuda, J. Hasegawa, M. Ishida, T. Nakajima, Y. Honda, O. Kitao, H. Nakai, T. Vreven, J. A. Montgomery Jr., J. E. Peralta, F. Ogliaro, M. Bearpark, J. J. Heyd, E. Brothers, K. N. Kudin, V. N. Staroverov, R. Kobayashi, J. Normand, K. Raghavachari, A. Rendell, J. C. Burant, S. S. Iyengar, J. Tomasi, M. Cossi, N. Rega, J. M. Millam, M. Klene, J. E. Knox, J. B. Cross, V. Bakken, C. Adamo, J. Jaramillo, R. Gomperts, R. E. Stratmann, O. Yazyev, A. J. Austin, R. Cammi, C. Pomelli, J. W. Ochterski, R. L. Martin, K. Morokuma, V. G. Zakrzewski, G. A. Voth, P. Salvador, J. J. Dannenberg, S. Dapprich, A. D. Daniels, Ö. Farkas, J. B. Foresman, J. V. Ortiz, J. Cioslowski, D. J. Fox, Gaussian, Inc., Wallingford CT, 2009.
- [27] a) A. D. Becke, *J. Chem. Phys.* **1993**, *98*, 5648-5652; b) C. Lee, W. Yang, R. G. Parr, *Phys. Rev. B* **1998**, *37*, 785-789; c) S. H. Vosko, L. Wilk, M. Nusair, *Can. J. Phys.* **1980**, *58*, 1200-1211.
- [28] S. Grimme, J. Antony, S. Ehrlich, H. Krieg, *J. Chem. Phys.* **2010**, *132*, 154104-154119.
- [29] F. Weigend, R. Ahlrichs, *Phys. Chem. Chem. Phys.* **2005**, *7*, 3297-3305.
- [30] a) S. Miertuš, E. Scrocco, J. Tomasi, *Chem. Phys.*, **1981**, *55*, 117-129; b) J. L. Pascual-Ahuir, E. Silla, I. Tuñón, *J. Comp. Chem.*, **1994**, *15*, 1127-1138; c) V. Barone, M. Cossi, *J. Phys. Chem. A*, **1998**, *102*, 1995-2001.
- [31] J. W. McIver, A. K. Komornicki, *J. Am. Chem. Soc.* **1972**, *94*, 2625-2633.
- [32] C. González, H. B. Schlegel, *J. Phys. Chem.* **1990**, *94*, 5523-5527.

## Entry for the Table of Contents

## RESEARCH ARTICLE

A new methodology for the synthesis of tetrahydroquinolines based on the transition metal-catalyzed intramolecular carbene C–H functionalization of  $\alpha$ -diazoesters is reported. Both the first generation Grubbs complex and  $[(\text{IMes})\text{Pd}(\text{NQ})]_2$  proved suitable for this purpose, the former being the most effective catalyst.



*Daniel Solé,\* Arianna Amenta, M.-Lluïsa Bennasar and Israel Fernández\**

**Page No. – Page No.**

**Transition Metal-Catalyzed  
Intramolecular Carbene C<sub>sp3</sub>-H  
Functionalization of  $\gamma$ -Amino- $\alpha$ -  
diazoesters for the Synthesis of  
Tetrahydroquinolines**

WILEY-VCH